Journal of Organometallic Chemistry, 396 (1990) 33–47
Elsevier Sequoia S.A., Lausanne
JOM 21006

Mono- and bi-nuclear molybdenum complexes of 2,6-bis(diphenylphosphino)-*N*-methylaniline

A. Bart van Oort, Peter H.M. Budzelaar *, John H.G. Frijns

Koninklijke/Shell-Laboratorium, Amsterdam (Shell Research B.V.), Postbus 3003, 1003 AA Amsterdam (The Netherlands)

and A. Guy Orpen

School of Chemistry, The University of Bristol Cantock's Close, Bristol BS8 1TS (U.K.)

(Received March 23rd, 1990)

Abstract

The new ligand 2,6-bis(diphenylphosphino)-*N*-methylaniline (LH) has been prepared via repeated *o*-lithiation of lithium *N*-methyl-*N*-phenylcarbamate. Reaction of LH with $Mo(CO)_6$ gives [*P*,*N*-LH]$Mo(CO)_4$ (**1**) and (with an excess of $Mo(CO)_6$) [μ-*P*,*N*: *P'*-LH][$Mo(CO)_4$][$Mo(CO)_5$] (**3**). Reaction of the anion L^- with $Mo(CO)_6$ initially gives the carbamoyl complex $\{[P,C\text{-LC(O)}]Mo(CO)_4\}^-Li^+$ (**4**), but use of an excess of $Mo(CO)_6$ and extended reaction times results in formation of the binuclear complex $\{[\mu\text{-}P,N: P',N\text{-L}][Mo(CO)_4]_2\}^-Li^+$ (**5**). Complex **5** does not react with oxygen, but treatment with halogen sources (CCl_4, Br_2, I_2) gives [μ-*P*,*N*: *P'*,*N*-L][μ-X][$Mo(CO)_3$]$_2$ (**6**, X = Cl, Br, I) via an intermediate formulated as $\{[\mu\text{-}P,N: P',N\text{-L}][Mo(CO)_4][Mo(CO)_3X_2]\}^-Li^+$ (**7**). All complexes have been characterized by ^{13}C and ^{31}P NMR spectroscopy. The structure of **6**-Br has been confirmed by a single-crystal X-ray diffraction study. The molecule of **6**-Br is of approximate C_s symmetry; each molybdenum atom is surrounded by three carbonyl groups, a phosphine, bridging nitrogen and bromine atoms (Mo–N = 2.18 and Mo–Br = 2.70 Å av.) and the second molybdenum atom (Mo–Mo = 2.987(2) Å). The metal–metal distance and electron-counting rules indicate the presence of a single metal–metal bond.

Introduction

In recent years, ligands capable of keeping two or more metals in close proximity have received considerable attention, primarily because of their potential applications in homogenous catalysis [1]. The most popular binucleating ligands are probably the neutral ligands bis(diphenylphosphino)methane (DPPM) [1a,b] and

0022-328X/90/$03.50

2-diphenylphosphinopyridine [2], and the anionic phosphido [3] and thiolato [4] groups. These bridging ligands are frequently capable of preserving the binuclear framework during reactions, but numerous exceptions have also been reported [5]. We were interested in designing a ligand system which holds it metal atoms so strongly that there is little chance of fragmentation during chemical transformations. The 2,6-bis(diphenylphosphino)-*N*-methylaniline ligand LH and especially its anion L^- (which should be capable of forming nitrogen-bridged bis(chelate) complexes) were thought likely meet to this requirement. In the present paper, we describe a simple one-pot synthesis of this new ligand. In order to explore its coordination chemistry, we have also prepared a number of mononuclear and binuclear molybdenum complexes.

Results and discussion

Ligand synthesis

2,6-Bis(diphenylphosphino)-*N*-methylaniline (LH) was prepared by the general procedure for electrophilic substitution of *N*-alkylanilines described by Katritzky [6] (Scheme 1). *N*-methylaniline was converted into the lithium carbamate, *o*-lithiated with ^{t}BuLi, treated with Ph_2PCl, *o*-lithiated again, and treated with a second equivalent of Ph_2PCl. Hydrolysis of the final carbamate produced the diphosphinoaniline in fair ($\approx 50\%$) yield. It is also possible to prepare the monophosphinoaniline by hydrolysis of the intermediate monophosphinocarbamate; this hydrolysis is much faster than that of the diphosphino analogue.

Reaction of LH with $Mo(CO)_6$

Refluxing of a THF solution of LH with ≤ 1 equivalent of $Mo(CO)_6$ gives pure [*P*,*N*-LH]$Mo(CO)_4$ (**1**). No intermediates are detected under the reaction conditions, although [*P*-LH]$Mo(CO)_5$ (**2**) is probably formed first (vide infra). With an excess of $Mo(CO)_6$ and longer reaction times, [μ-*P*,*N*: *P'*-LH][$Mo(CO)_4$][$Mo(CO)_5$] (**3**) is obtained. NMR data for these complexes are in Tables 1 (^{31}P) and 2 (^{13}C).

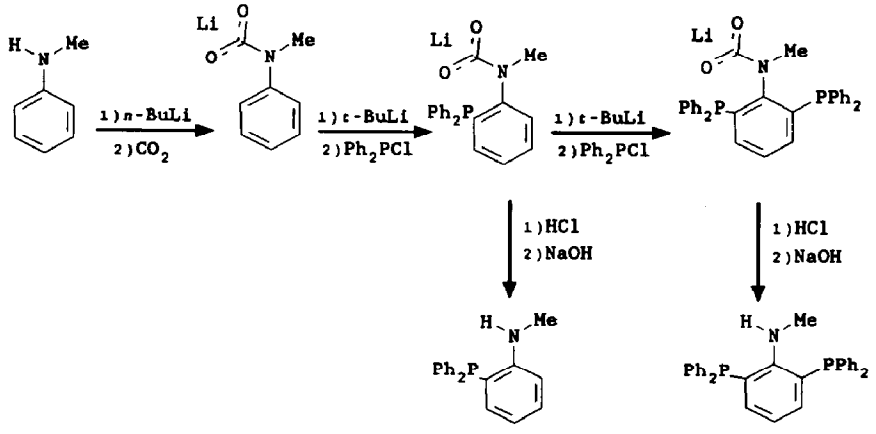

Scheme 1. Synthesis of *o*-phosphino-*N*-alkylanilines.

Table 1

^{31}P NMR data

Compound	δP (ppm)	J(PP) (Hz)
LH	−14.0	8 [a]
1	40.3, −20.9	9
2	−11.4, 32.6	4
3	41.0, 36.6	3
4	46.4, −4.3	4
5	39.8	12 [a]
6-Cl	46.9	12 [a]
6-Br	45.9	12 [a]
6-I	43.8	12 [a]
7	75.3,34.6	~0

[a] Determined from the ^{13}C spectrum.

Reaction of L^- with $Mo(CO)_6$

The lithium amide LLi is easily prepared from LH and ^{n}BuLi in THF at −40 °C. It reacts smoothly with $Mo(CO)_6$ to give an extremely air- and moisture-sensitive complex which was identified as **4** on the basis of ^{1}H, ^{13}C and ^{31}P NMR data. Carbamoyl complex **4** is probably formed by attack of the amido nitrogen on a carbon monoxide ligand of $Mo(CO)_6$, followed by displacement of a carbonyl by phosphine. There are precedents for such amide-carbonyl coupling reactions, although the products are frequently unstable [7]. In the present case, the extra stability conferred by the chelate ring structure may be important.

Controlled hydrolysis of **4** gave **2**, which loses CO to give **1** with a half-life of ca. $1\frac{3}{4}$ hour at room temperature. NMR data for **2** are included in Tables 1 and 2. Apparently, the CO elimination and ring closure of **2** to give **1** is more rapid than the formation of **2** from LH and $Mo(CO)_6$, so it is not surprising that **2** was not detected as an intermediate in the preparation of **1** as described above.

Refluxing of **4** with an excess of $Mo(CO)_6$ for at least 1 day gives the symmetrical anion $\{[\mu\text{-}P,N\text{: }P',N\text{-L}][Mo(CO)_4]_2\}^-$ (**5**) in which the carbamoyl carbonyl has been lost. Inspection of CPK models suggests that this loss of CO from **4** must

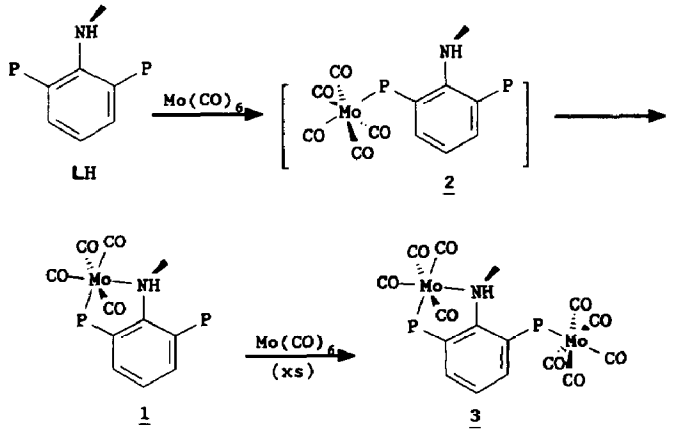

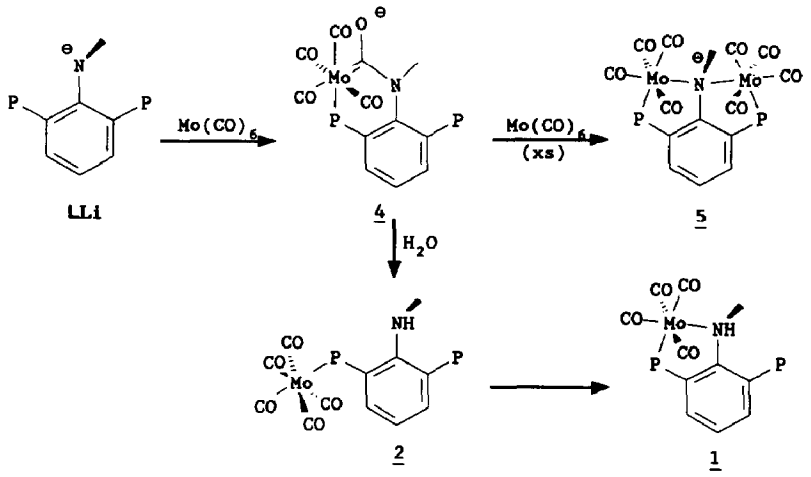

occur before coordination of a molybdenum fragment to the free phosphorus atom can take place: in **4**, the *N*-methyl group is pushed into the phosphorus lone pair and prevents Mo–P coordination. The steric congestion around this phosphorus atom should be much less in the $\{[P,N\text{-L}]Mo(CO)_4\}^-$ anion obtained by CO loss from **4**. Since the formation of carbamoyl complexes is often reversible [7b], C–N dissociation followed by CO loss and Mo–N bond formation seems a plausible mechanism for this reaction.

Oxidation of $\{[\mu\text{-}P,N:P',N\text{-L}][MoCO)_4]_2\}^-$ *(6)*

The lithium salt **5** is a red solid, very sensitive to proton sources; it does not react with simple olefins and acetylenes. Surprisingly, **5** is not sensitive to oxygen, but it reacts rapidly with halogen sources (CCl_4, Br_2, CH_2I_2, I_2). The final product of these reactions is $[\mu\text{-}P,N:P',N\text{-L}][\mu\text{-X}][Mo(CO)_3]_2$ (**6**, X = Cl, Br, I); the bromide was characterized by X-ray diffraction (vide infra). We have attempted to follow these reactions by NMR spectroscopy. The clearest results were obtained in the CCl_4 oxidation: Fig. 1 shows a series of ^{31}P spectra for this reaction at various temperatures. Solutions of the reactants were mixed in a high-pressure NMR tube at low temperature, and the temperature was raised slowly. The starting material shows a sharp singlet at 37.0 ppm, and this became very broad at −30 °C. Two resonances (at 75.0 and 34.9 ppm) of an intermediate **7** grew in at ca. −20 °C. At 0 °C, virtually all of the starting material had been converted into this intermediate; a ^{13}C spectrum recorded at this point showed a species with seven distinct carbonyl resonances. When the temperature was raised further, a new singlet (due to **6**-Cl) appeared in the ^{31}P spectrum at 47.1 ppm, and the two peaks due to **7** gradually disappeared. The Br_2 and I_2 oxidations followed similar patterns, but the intermediates decomposed faster, and no satisfactory ^{13}C spectra could be recorded. On the basis of the ^{13}C and ^{31}P NMR data, intermediate **7** is suggested to have the formula $\{[\mu\text{-}P,N:P',N\text{-L}][Mo(CO)_4][Mo(CO)_3X_2]\}^-Li^+$, with the dispositions of the chlorine and carbonyl ligands around Mo^{II} uncertain [8*]. Some NMR data for

* Reference number with asterisk indicates a note in the list of references.

7 are included in Tables 1 and 2, although the quality of the spectra was insufficient to allow assignment of the ^{13}C signals in the aromatic region.

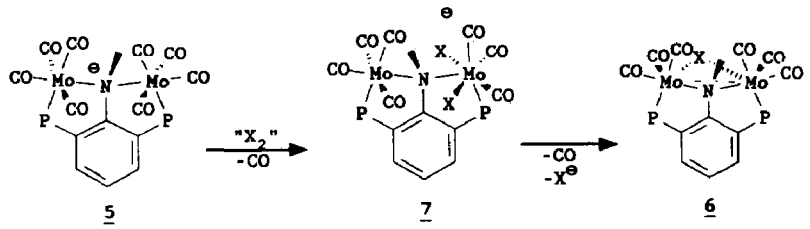

Crystal structure of [μ-P,N : P′,N-L][μ-Br][Mo(CO)$_3$]$_2$ (6-Br)

Figure 2 shows two views of the structure of **6**-Br. The top view (2a) clearly shows that each molybdenum atom is surrounded by three carbonyl groups, one

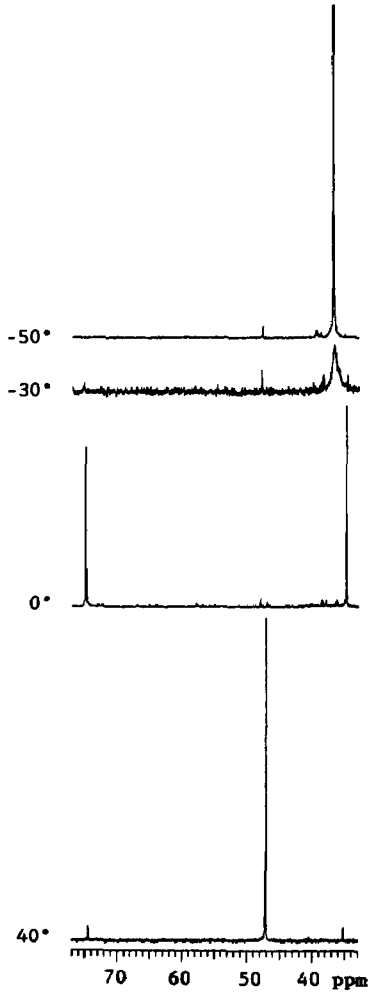

Fig. 1. ^{31}P NMR spectra showing the oxidation of **5** with CCl_4 to give **6**-Cl via **7**.

phosphorus atom, the bridging nitrogen and bromine atoms, and the second molybdenum; Table 3 contains important bond lengths and angles. Both the metal–metal distance (2.987(2) Å; cf. $(\mu\text{-I})_2[Mo(CO)_4]_2$ [9] and $(\mu\text{-I})_2[W(CO)_4]_2$ [10], M–M = 3.16 Å) and the total electron count are consistent with the presence of a single Mo–Mo bond. We have also carried out extended-Hückel calculations [11] on the model system $(\mu\text{-NH}_2)(\mu\text{-Br})[Mo(CO)_3PH_3]_2$, and the results support the presence of a direct metal–metal bond. The SOMO of the $Mo(CO)_3PH_3^+$ radical is largely Mo $d_{x^2-y^2}$ in character. When two of these radicals are combined, the in-phase combination of these fragment SOMO's produces a single metal–metal σ-bond, which is largely unaffected by the addition of the bridging NH_2^- and Br^- groups. This metal–metal bonding orbital is shown in Fig. 3.

The X-ray structure (Fig. 2a) also illustrates the crowding of the carbonyl groups *trans* to phosphorus: these groups are significantly distorted from linearity (MoCO = 168(1) and 169(1)°) to avoid a close O–O contact (O(1) · · · O(6) = 2.83(2) Å; C(1) · · · C(6) = 2.59(2) Å). The side view (2b) shows the out-of-plane deformation of the phosphorus atoms from the aniline ring plane, which enables the formation of the nitrogen and bromine bridges (and the Mo–Mo bond) with retention of the

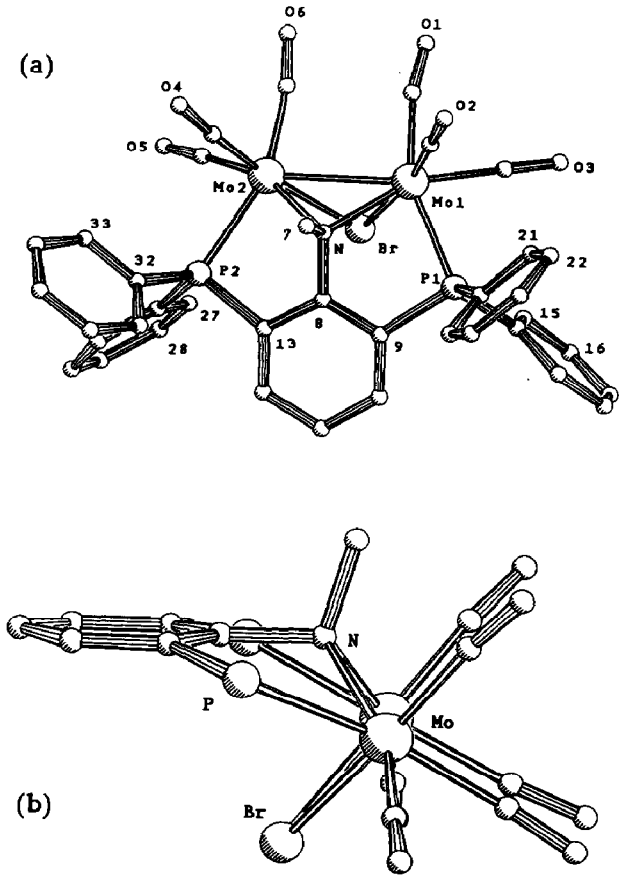

Fig. 2. PLUTO drawings of 6-Br. (a) Top via, showing the atom numbering. (b) Side view, showing the out-of-plane bending of the phosphorus atoms (phenyl groups have been omitted for clarity).

strong Mo–P bonds. Figure 2b also shows that the Mo(1)–N–Mo(2) and Mo(1)–Br–Mo(2) planes are nearly perpendicular (105.8°), in contract with the planar M_2X_2 arrangement found in $(\mu\text{-I})_2[M(CO)_4]_2$ complexes [9,10]. In a hypothetical coplanar structure, the geometric constraints imposed by the diphosphinoaniline ligand would cause the two $Mo(CO)_3$ units to adopt a *mer*-geometry rather than the *fac*-geometry observed here. The preference for *fac*-isomers in 18-electron $ML_3(CO)_3$ species is well-known, and is usually ascribed to the possibility of stabilization of all three metal t_{2g} orbitals by π-backbonding to CO; a similar argument could be advanced here. No such distinction applies in the case of $(\mu\text{-I})_2[M(CO)_4]_2$, where the arrangements of the CO ligands around the metal atoms would be the same for the coplanar and perpendicular structures. Presumably, the preference for a coplanar structure in that case is dictated by the reduction of unfavourable I · · · I non-bonded interactions that such an arrangement allows.

NMR spectroscopy of [μ-P,N:P',N-L][μ-X][Mo(CO)$_3$]$_2$ (6)

The ^{13}C NMR spectra of the complexes **6** feature only a single broad resonance for the carbonyl carbons at room temperature. At −70 °C, the bromide (**6**-Br) shows three well-separated carbonyl resonances; these are still too broad to distinguish any phosphorus couplings, so we cannot assign them with certainty. The fluxionality of the complexes of **6** is consistent with their formulation as 7-coordinate complexes [12]; also, the strong repulsion between O(1) and O(6) should favour pseudorotation.

One final feature of the ^{13}C spectra of compounds **6** (X = Cl–I) is worth noting. In the room-temperature spectra, the resonance due to carbon atoms C(9) and C(13)

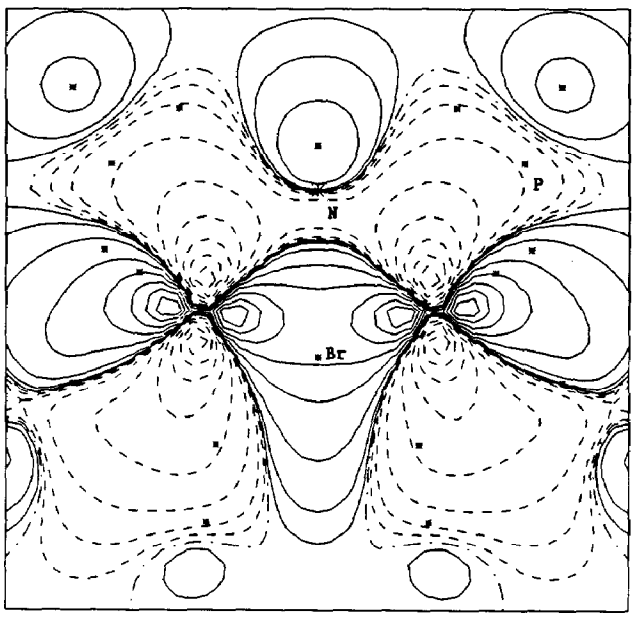

Fig. 3. View of the metal–metal bonding orbital of $(\mu\text{-NH}_2)(\mu\text{-Br})[Mo(CO)_3PH_3]_2$ in the plane containing the Mo and N atoms; projections of the other atoms on the cross-section are indicated by asterisks.

Table 2

^{13}C NMR data: δ, ppm (J(PC), Hz)

Compound	X	A	B	C_1	C_2	C_3	C_4	C_5	C_6	CH_3
LH	H	–	–	158.4(18)	131.0(13,2)	136.3(–)	123.3(–)			37.8(9)
1	H	$Mo(CO)_4$	–	158.8(19,22)	131.8(27,2)	134.4(–)	127.4(4)	136.1(1,1)	133.0(16,6)	49.9(6)
2	H	–	$Mo(CO)_5$	156.9(22,8)	132.6(18,4)	139.8(–)	123.1(8)	135.2(22)	127.6(35,3)	37.5(16)
3	H	$Mo(CO)_4$	$Mo(CO)_5$	156.9(23,1)	132.0(25,6)	136.1(1)	127.0(10,4)	135.7(17,1)	134.4(27,3)	49.5(–)
4	(Li salt)	$Mo(CO)_4CO$	–	157.5(23,12)	137.8(37,8)	143.1(18)	124.6(6)	135.8(15)	135.7(19,4)	37.8(20)
5	(Li salt)	$Mo(CO)_4$	$Mo(CO)_4$	185.1(26)	133.0(~ 30)	136.6(–)	121.6(4)			71.4(–)
6-Cl	–	$Mo(CO)_3$–Cl–$Mo(CO)_3$		177.1(30)	140.6(37,6)	138.6(2)	132.2(5)			66.5(–)
6-Br	–	$Mo(CO)_3$–Br–$Mo(CO)_3$		177.4(29)	139.2(36,7)	138.4(3)	131.8(5)			68.2(–)
6-I	–	$Mo(CO)_3$–I–$Mo(CO)_3$		178.5(29)	141.5(35,9)	137.7(2)	131.4(5)			70.5(–)
7	(Li salt)	$Mo(CO)_3Cl_2$	$Mo(CO)_4$	179.8(27,23)	[a]					

	Carbonyls *trans* to N	*trans* to P(A)	*cis*(A)	carbamoyl	*trans* to P(*B*)	*cis* (*B*)
1	221.0(7)	215.9(33)	207.7(9),208.8(9)			
2					211.7(23)	206.7(9)
3	220.7(7)	215.2(33)	206.7(9),209.7(9)		209.2(25)	205.2(8)
4	222.9(9)	224.2(29)	212.1(9),214.6(9)	233.7(20)		
5	225.3(9)	220.5(40)	210.5(7) (2×)			
6-Cl	228.6(br) [c]					
6-Br	228.0(br) [b,c]					
6-I	227.0(br) [b]					
7	227.4(9)	220.1(25)	203.9(8),204.4(8)		203.0(35)	218.4(16),219.6(11)

[a] The quality of the low-temperature spectrum was not sufficient to assign the remaining 25 signals in the aromatic region (128.5–136.5 ppm). [b] At room temperature. [c] Three separate (broad) signals were observed at $-70\,^{\circ}C$: 218, 228 and 236 ppm.

Table 3

Selected geometry data for **6**-Br

Bond lengths (Å)							
Mo1–Mo2	2.987(2)	Mo1–Br	2.690(2)	Mo1–P1	2.515(4)	Mo1-N	2.181(9)
Mo1–C1	2.00(2)	Mo1–C2	1.96(1)	Mo1–C3	1.99(1)	Mo2–Br	2.707(2)
Mo2–N	2.176(9)	Mo2–P2	2.514(3)	Mo2–C4	1.92(1)	Mo2–C5	2.00(2)
Mo2–C6	2.00(1)	P1–C9	1.82(1)	P1–C14	1.81(1)	P1–C20	1.81(1)
P2–C13	1.83(1)	P2–C26	1.82(1)	P2–C32	1.81(1)	O1–C1	1.14(2)
O2–C2	1.15(2)	O3–C3	1.15(2)	O4–C4	1.1791)	O5–C5	1.13(2)
O6–C6	1.15(2)	N–C7	1.51(1)	N–C8	1.46(1)	C8–C9	1.38(2)
C8–C13	1.40(2)	C9–C10	1.35(2)	C10–C11	1.39(2)	C11–C12	1.41(2)
C12–C13	1.38(2)	Cl · · · C6	2.59(2)	O6 · · · O1	2.83(2)		

Bond angles (°)					
Mo2–Mo1–Br	56.66(5)	Mo2–Mo1–P1	116.92(9)	Mo2–Mo1–N	46.6(2)
Mo2–Mo1–Cl	84.2(4)	Mo2–Mo1–C2	112.9(4)	Mo2–Mo1–C3	149.3(4)
Br–Mo1–P1	93.56(9)	Br–Mo1–N	77.8(2)	Br–Mo1–C1	93.6(4)
Br–Mo1–C2	169.5(4)	Br–Mo1–C3	100.6(3)	P1–Mo1N	75.6(2)
P1–Mo1–C1	158.1(4)	P1–Mo1–C2	90.9(4)	P1–Mo1–C3	81.8(4)
N–Mo1–C1	126.2(5)	N–Mo1–C2	94.1(4)	N–Mo1–C3	157.1(4)
C1–Mo1–C2	85.8(5)	C1–Mo1–C3	76.6(6)	C2–Mo1–C3	89.5(5)
Mo1–Mo2–Br	56.13(5)	Mo1–Mo2–N	46.8(2)	Mo1–Mo2–P2	118.04(9)
Mo1–Mo2–C4	114.3(3)	Mo1–Mo2–C5	144.6(4)	Mo1–Mo2–C6	84.5(4)
Br–Mo2–N	77.5(2)	Br–Mo2–P2	95.71(9)	Br–Mo2–C4	170.4(3)
Br–Mo2–C5	96.5(4)	Br–Mo2–C6	95.8(4)	N–Mo2–P2	75.9(2)
N–Mo2–C4	96.0(4)	N–Mo2–C5	157.7(5)	N–Mo2–C6	125.7(4)
P2–Mo2–C4	89.4(3)	P2–Mo2–C5	83.5(4)	P2–Mo2–C6	157.4(4)
C4–Mo2–C5	92.2(5)	C4–Mo2–C6	82.3(5)	C5–Mo2–C6	75.9(6)
Mo1–Br–Mo2	67.21(5)	Mo1–P1–C9	99.8(4)	Mo2–P2–C13	98.9(4)
Mo1–N–Mo2	86.6(3)	Mo1–N–C7	116.6(6)	Mo1–N–C8	114.7(6)
Mo2–N–C7	117.4(6)	Mo2–N–C8	114.7(6)	C7–N–C8	106.3(8)
Mo1–C1–O1	168.0(1)	Mo1–C2–O2	174.0(1)	Mo1–C3–O3	179.0(1)
Mo2–C4–O4	175.0(1)	Mo2–C5–O5	179.0(1)	Mo2–C6–O6	169.0(1)
N–C8–C9	121.1(9)	N–C8–C13	120.0(1)	C9–C8–C13	119.0(1)
P1–C9–C8	113.0(8)	P1–C9–C10	126.0(1)	C8–C9–C10	120.0(1)
C9–C10–C11	122.0(1)	C10–C11–C12	118.0(1)	C11–C12–C13	119.0(1)
P2–C13–C8	113.8(8)	P2–C13–C12	124.4(9)	C8–C13–C12	121.0(1)

Distances to least-squares plane through C8 · · · C13 (Å)										
C8	−0.01(8)	C9	0.02(8)	C10	0.02(8)	C11	−0.02(8)	C12	0.03(8)	C13	0.01(8)
N1	−0.02(8)	P1	0.34(8)	P2	0.32(7)						

of the aniline ring is split into an 8-line pattern (Fig. 4a) instead of the 6-line pattern expected for the AXX′ system of one ^{13}C and two ^{31}P nuclei [13]. Six of these lines have the positions expected for the pure AXX′ system, although the intensities of the outer lines are too large. In the low-temperature spectrum (Fig. 4b) the "spurious" lines have broadened and disappeared in the baseline noise. This curious behaviour is not related to the fluxional behaviour of the molecule, but is due to the presence of magnetically active Mo nuclei. Molybdenum contains 9.5% ^{97}Mo and 15.7% ^{95}Mo (both spin 5/2; the other naturally occurring isotopes have spin 0). ^{97}Mo has a high quadrupole moment and relaxes rapidly in all but the most

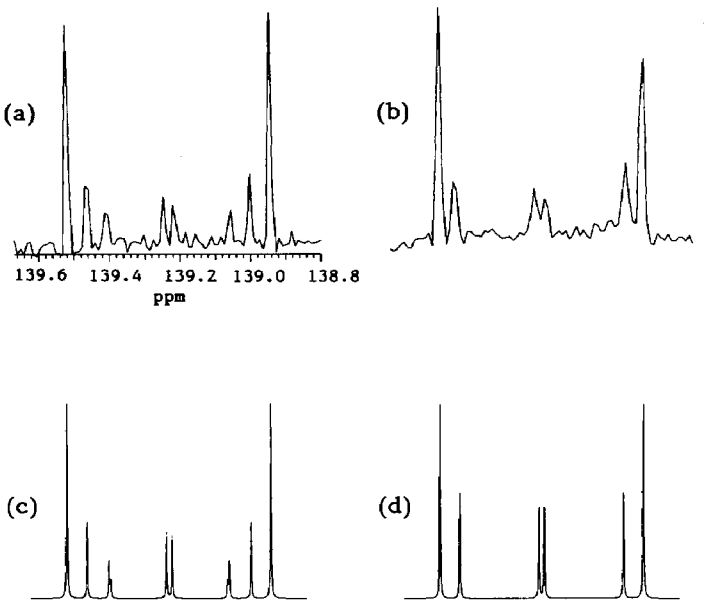

Fig. 4. ^{13}C NMR signal of the carbon atoms C9 and c13 of **6**-Br at (a) room temperature and (b) $-70\,^{\circ}C$; simulated spectra with (c) and without (d) coupling to ^{95}Mo.

symmetric complexes, so that it effectively behaves as a spin 0 nucleus. The quadrupole moment of ^{95}Mo is not very large, however, and couplings to it are frequently observed. If either of the two molybdenum atoms in **6** is ^{95}Mo, the $^{1}J(MoP)$ (normally in the range of 90–250 Hz [14]) can introduce a very large effective shift difference between the phosphorus atoms. Thus, the observed pattern is a superposition of one AXX′ and one AMX pattern, of which the outer lines coincide (Fig. 4c) [15*]. If the temperature is lowered, the quadrupole relaxation of ^{95}Mo becomes faster, the $^{1}J(MoP)$ coupling is lost, and the normal AXX′ pattern is restored (Fig. 4d) [16*].

Conclusions

The new ligand L^- can, indeed, form stable nitrogen-bridged bis(chelate) complexes. The robustness of this system is clearly illustrated by the reaction of **5** with an excess of bromine, which results only in oxidation at the metal, even though free anilines undergo rapid ring halogenation with bromine. Therefore, we can expect the diphosphinoaniline system to be capable of holding together metal atoms even under the relatively drastic conditions necessary for many chemical reactions.

Experimental

2,6-Bis(diphenylphosphino)-N-methylaniline (LH)

A stirred solution of 46 mmol of *N*-methylaniline in 100 ml of THF was cooled to $-70\,^{\circ}C$, and 29 ml $^{n}BuLi$ (1.6 *M* in hexane; 46 mmol) was added dropwise. The cooling bath was then removed and the temperature was allowed to rise to $0\,^{\circ}C$. Carbon dioxide was bubbled through the solution for a few minutes; this resulted in

a marked rise in temperature. The solvent was removed in vacuo, and 100 ml of THF was added. The resulting solution of the lithium carbamate was cooled to −70 °C, and ^{t}BuLi (38 ml of 1.4 *M* solution in hexanes; 53 mmol) was added dropwise to the stirred solution. The temperature was then allowed to rise to −20 °C and kept there for 30 min. The solution was again cooled to −70 °C, and 9 ml of Ph_2PCl (50 mmol) in 20 ml of THF was added with stirring. The solution was slowly warmed to 0 °C, then cooled again to −70 °C, and the addition of ^{t}BuLi and Ph_2PCl repeated. After this second addition, the temperature was again raised to 0 °C, and the solvents were removed in vacuo. Then, 100 ml of THF and 50 ml of 2 *M* HCl were added, resulting in a visible evolution of CO_2. After 30 min the solution was made strongly alkaline with concentrated aqueous NaOH. A few minutes later, the THF layer was separated and the aqueous layer was extracted with two 50-ml portions of THF. The THF was removed in vacuo and the residue was crystallized from ethanol containing a little THF (yield: 55%).

[P,N-LH]Mo(CO)$_4$ (1)

A mixture of 475 mg (1 mmol) LH and 264 mg (1 mmol) molybdenum hexacarbonyl in 50 ml of toluene was refluxed for 2 h then cooled to room temperature and the solvent evaporated. The residual solid was washed with hexane and dried in vacuo.

[μ-P,N: P′-LH][Mo(CO)$_4$][Mo(CO)$_5$] (3)

A mixture of 570 mg (1.2 mmol) LH and 665 mg (2.52 mmol) molybdenum hexacarbonyl in 50 ml of toluene was refluxed for 4 h then cooled to room temperature and the solvent removed in vacuo. The residue was washed with hexane and the (yellow) product dried in vacuo.

[P,C-LC(O)]Mo(CO)$_4$Li (4)

A stirred solution of 950 mg (2 mmol) LH in 50 ml of THF was cooled to −78 °C and 1.25 ml ^{n}BuLi solution (1.6 *M* in hexane; 2 mmol) was added dropwise. The mixture, which turned orange-red, was allowed to warm to room temperature and 528 mg (2 mmol) of molybdenum hexacarbonyl were added, and the mixture refluxed for 1 h then cooled to room temperature. The dark red solution was evaporated to dryness and the residue recrystallized from toluene/THF as small yellow crystals.

[μ-P,N: P′,N-L][MoCO)$_4$]$_2$Li (5)

A stirred solution of 4.75 g (10 mmol) of LH in 50 ml of THF was cooled to −78 °C, and 6.25 ml of a ^{n}BuLi solution (1.6 *M* in hexane, 10 mmol) were added dropwise; The mixture turned orange-red. The mixture was allowed to warm to room temperature. Then, 5.28 g (20 mmol) of molybdenum hexacarbonyl were added, and the mixture was refluxed for 18 h then allowed to cool to room temperature. The solvent was removed, leaving the dark red complex **5**.

[μ-P,N: P′,N-L][μ-Br][Mo(CO)$_3$]$_2$ (6-Br)

A stirred solution of 3.69 g (4 mmol) of [μ-*P*,*N*: *P*′,*N*-L][Mo(CO)$_4$]$_2$Li (**5**) in 75 ml of THF was cooled to −78 °C, and 0.64 g (8 mmol) of bromine were added. The colour immediately changed from clear red to dark green and then, with evolution

of CO, to very dark red. The mixture was allowed to warm to room temperature; release of CO was again observed and the colour changed to dark green. The solvent was evaporated, 50 ml of water were added to the residue, and the mixture was extracted with dichloromethane. The organic fraction was dried over magnesium sulphate and the solvent removed in vacuo. The product (**6**-Br) was crystallized from THF/ether as small dark-green crystals (86% yield).

NMR monitoring of the oxidation of **5** *with* CCl_4

A solution of 90 mg (0.1 mmol) [μ-*P*,*N*: *P*′,*N*-L][$Mo(CO)_4$]$_2$Li (5) in 3 ml $CDCl_3$ was prepared in a sapphire high-pressure NMR tube at $-78\,^\circ$C, and 0.5 ml CCl_4 was added. The reaction was monitored by NMR spectroscopy, starting at $-50\,^\circ$C. Raising the temperature to $-30\,^\circ$C resulted in a broadening of the sharp singlet of **5** ($\delta = 37.0$ ppm) in the ^{31}P spectrum. At $0\,^\circ$C, the first stage of the reaction was complete and the ^{31}P spectrum showed only the two resonances of intermediate **7** ($\delta = 75.0$ and 34.9 ppm). The NMR tube was cooled to $-30\,^\circ$C to suppress further reaction, and a ^{13}C spectrum was recorded. After this, the temperature was raised to $20\,^\circ$C, resulting in the gradual disappearance of **7** and the formation of **6**-Cl ($\delta = 47.1$ ppm).

X-ray structure determination of **6**-Br

$C_{37}H_{26}BrMo_2O_6P_4$, $M_w = 976.3$, monoclinic $P2_1/c$ (No. 14), $a = 11.385(3)$, $b = 21.398(6)$, $c = 14.696(5)$ Å, $\beta = 91.08(3)\,^\circ$, $U = 3580(2)$ Å^3, $Z = 4$, $D_c = 1.81$ g/cm^3, $\lambda = 0.71069$ Å, μ(Mo-K_α) = 18.8 cm^{-1}, $F(000) = 1808$, $T = 295$ K. Crystal faces [distances in mm from origin] (1 0 0) [0.045], (−1 0 0) [0.045], (0 1 0) [0.040], (0 −1 0) [0.040], (0 0 1) [0.14], (0 0 −1) [0.14]; minimum and maximum transmission coefficients: 0.838, 0.870.

A single crystal of **6**-Br (approx. dimensions 0.08 × 0.09 × 0.28 mm) was mounted in a thin-walled glass capillary under nitrogen. All diffraction measurements were made on a Nicolet P3m diffractometer at room temperature, using graphite monochromated Mo-K_α X-radiation. Unit cell dimensions were determined from 15 centered reflections in the range $25.0 < 2\theta < 27.0\,^\circ$. A total of 5846 diffracted intensities were measured in a unique quadrant of reciprocal space for $4.0 < 2\theta < 50.0\,^\circ$ by Wyckoff ω scans. For $40 < 2\theta < 50\,^\circ$, reflections with intensity < 20 cs^{-1} were not recorded. Three check reflections re-measured after every 50 ordinary data showed no significant decay but ca. 3% variation over the period of data collection; an appropriate correction was therefore applied. Of the intensity data collected, 4067 unique observations remained after averaging of duplicate and equivalent measurements and deletion of systematic absences; of these, 2547 with $I > 3\sigma(I)$ were retained for use in structure solution and refinement. An absorption correction was applied on the basis of the indexed crystal faces, and the data were corrected for Lorentz and polarization effects.

The structure was solved by conventional heavy-atom (Patterson and Fourier) methods; all calculations were carried out on a Nicolet R3m/V structure determination system using programs of the SHELXTL-PLUS package [17]. Complex neutral-atom scattering factors were taken from reference [18]. All atoms heavier than carbon were assigned anisotropic thermal parameters, all carbons were refined isotropically, and all hydrogens were assigned a fixed thermal parameter of 0.06 Å^2. All non-hydrogen atoms were refined without positional constraints; hydrogen atoms were

Table 4

Final positional end equivalent thermal parameters for **6-Br**

Atom	x	y	z	U_{eq}
Mo1	0.8528(1)	0.36293(5)	0.14049(7)	0.0293(4)
Mo2	0.6680(1)	0.26403(5)	0.12949(7)	0.0296(4)
Br	0.7738(1)	0.30138(6)	0.28673(8)	0.0397(5)
P1	1.0612(3)	0.3269(1)	0.1655(2)	0.034(1)
P2	0.7319(3)	0.1518(1)	0.1413(2)	0.031(1)
O1	0.653(1)	0.4633(5)	0.138(1)	0.125(7)
O2	0.9102(9)	0.4217(5)	−0.0464(6)	0.068(4)
O3	0.954(1)	0.4843(5)	0.2312(7)	0.092(5)
O4	0.5645(8)	0.2407(4)	−0.0630(5)	0.053(3)
O5	0.438(1)	0.2126(5)	0.2161(9)	0.100(5)
O6	0.4801(9)	0.3704(4)	0.1091(7)	0.071(4)
N	0.8525(8)	0.2662(4)	0.0938(5)	0.027(3)
C1	0.716(1)	0.4219(7)	0.136(1)	0.061(4)
C2	0.892(1)	0.3971(6)	0.0213(8)	0.041(3)
C3	0.916(1)	0.4398(6)	0.1990(8)	0.044(3)
C4	0.609(1)	0.2480(5)	0.0085(8)	0.037(3)
C5	0.521(1)	0.2319(7)	0.1855(9)	0.057(4)
C6	0.556(1)	0.3359(6)	0.1206(8)	0.044(3)
C7	0.882(1)	0.2554(5)	−0.0046(7)	0.038(3)
C8	0.928(1)	0.2243(5)	0.1469(7)	0.032(3)
C9	1.037(1)	0.2433(5)	0.1789(7)	0.034(3)
C10	1.105(1)	0.2036(6)	0.2276(8)	0.051(4)
C11	1.071(1)	0.1427(7)	0.2468(9)	0.056(4)
C12	0.957(1)	0.1236(6)	0.2186(8)	0.048(4)
C13	0.888(1)	0.1642(5)	0.1679(7)	0.034(3)
C14	1.144(1)	0.3479(5)	0.2671(8)	0.039(3)
C15	1.088(1)	0.3611(6)	0.3464(9)	0.056(4)
C16	1.150(2)	0.3745(7)	0.428(1)	0.069(5)
C17	1.269(2)	0.3749(7)	0.427(1)	0.073(5)
C18	1.328(1)	0.3618(7)	0.3485(9)	0.064(4)
C19	1.268(1)	0.3473(6)	0.2684(9)	0.049(4)
C20	1.163(1)	0.3372(5)	0.0737(8)	0.037(3)
C21	1.181(1)	0.3985(6)	0.0420(9)	0.056(4)
C22	1.253(1)	0.4087(8)	−0.031(1)	0.074(5)
C23	1.304(2)	0.3597(8)	−0.073(1)	0.076(5)
C24	1.287(2)	0.3015(8)	−0.044(1)	0.078(5)
C25	1.216(1)	0.2887(7)	0.0300(9)	0.062(4)
C26	0.680(1)	0.1028(5)	0.2336(8)	0.036(3)
C27	0.660(1)	0.1309(6)	0.3164(8)	0.046(3)
C28	0.621(1)	0.0956(6)	0.3873(9)	0.051(4)
C29	0.602(1)	0.0328(6)	0.3769(9)	0.051(4)
C30	0.628(1)	0.0047(7)	0.2997(9)	0.066(4)
C31	0.665(1)	0.0387(7)	0.2233(9)	0.058(4)
C32	0.727(1)	0.1002(6)	0.0440(8)	0.042(3)
C33	0.824(1)	0.0715(6)	0.0093(9)	0.057(4)
C34	0.816(2)	0.0312(7)	−0.065(1)	0.078(5)
C35	0.711(2)	0.0204(7)	−0.103(1)	0.067(4)
C36	0.615(2)	0.0477(7)	−0.075(1)	0.073(5)
C37	0.620(1)	0.0886(7)	0.0011(9)	0.064(4)

constrained to idealised geometries (d(C–H) = 0.96 Å). Full-matrix least-squares refinement of this model (252 parameters) converged to final residual indices $R = 0.047$, $R_w = 0.051$, $S = 1.18$ [19*]. Weights w were set equal to $[\sigma_c^2(F_o) + gF_o^2]^{-1}$, where $\sigma_c^2(F_o)$ is the variance in F_o by counting statistics, and $g = 0.0005$ was chosen to minimize the variation in S as a function of F_o. Final difference electron density maps showed no features outside the range from +0.6 to −0.5 eÅ^{-3}, the largest of these being close to carbon atoms of the phenyl rings. Table 4 lists the final atomic coordinates and equivalent isotropic thermal parameters for the non-hydrogen atoms.

Supplementary material available. Tables of positional and thermal parameters, bond lengths and angles, and observed and calculated structure factors (15 pages) are available on request from one of the authors (PHMB).

References and notes

1 See e.g. (a) A.L. Balch in L.H. Pignolet (Ed.), Homogeneous Catalysis with Metal Phosphine Complexes, Plenum press, New York, 1983, p. 167; (b) A.R. Sanger, ibid., p. 216; (c) R.J. Puddephatt, Chem. Soc. Rev., (1983) 99.

2 See e.g. J.P. Farr, M.M. Olmstead and A.L. Balch, J. Am. Chem. Soc., 102 (1980) 6654; J.P. Farr, M.M. Olmstead, N.M. Rutherford, F.E. Wood and A.L. Balch, Organometallics, 2 (1983) 1758; G. Bruno, S. Lo Schavio, E. Rotondo, C.G. Arena and F. Faraone, Organometallics, 8 (1989) 886, and references cited therein.

3 See e.g. A.J. Carty, Adv. Chem. Ser. 196 (1982) 163; R. Whyman in B.F.G. Johnson (Ed.), Transition Metal Clusters, Wiley, New York, 1980, p. 545, and references cited therein.

4 See e.g. J.J. Bonnet, J. Galy, D. de Montauzon and R. Poilblanc, J. Chem. Soc., Chem. Commun., (1977) 47; J.A. de Beer, R.J. Haines, R. Greatrex and N.N. Greenwood, J. Chem. Soc. A, (1971) 3271.

5 See e.g. B. Delavaux, B. Chaudred, J. Devillers, F. Dahan, G. Commenges and R. Poilblanc, J. Am. Chem. Soc., 108 (1986) 3703; C. Bergounhou, J.J. Bonnet, P. Fompeyrine, G. Lavigne, N. Lugan and F. Mansilla, Organometallics, 5 (1986) 60; G. Lavigne, N. Lugan and J.J. Bonnet, ibid., 1 (1982) 1040; S. Rosenberg, G.L. Geoffroy and A.L. Rheingold, ibid., 4 (1985) 1184; P. Kalck, J.J. Bonnet and R. Poilblanc, J. Am. Chem. Soc., 104 (1982) 3069; N. Lugan, J.J. Bonnet and J.A. Ibers, Organometallics, 7 (1988) 1538; B.M. Mattson and L.N. Ito, ibid., 8 (1989) 391.

6 A.R. Katritzky, W.-Q. Fan and K. Akutagawa, Tetrahedron, 42 (1986) 4027.

7 (a) E.O. Fischer and H.J. Kollmeier, Angew. Chem., 82 (1970) 325; (b) r.J. Angelici, Acc. Chem. Res., 5 (1972) 335.

8 Formulated in this way, the first step of the oxidation parallels that of $Mo(CO)_5X^-$ to $Mo(CO)_4X_3^-$: R.B. King, Inorg. Chem., 3 (1964) 1039; M.C. Ganorkar and M.H.B. Stiddard, J. Chem. Soc., (1965) 3494. The NMR data for 7 unambiguously show it to contain seven carbonyl ligands, four on Mo^0 and three on Mo^{II}. This leaves open an alternative formulation as neutral [μ-P,N: P',N-L][$Mo(CO)_4$][$Mo(CO)_3X$], with a six-coordinate Mo^{II} atom. Such six-coordinate complexes are, however, usually paramagnetic (R. Colton and C.J. Rix, Aust. J. Chem., 21 (1968) 1155), so the structure shown in the next is the more likely one. Unfortunately, 7 loses CO so easily that it could not be isolated, and we were unable to settle this question.

9 G. Schmidt, R. Boese and E. Welz, Chem. Ber., 108 (1975) 260; R. Boese and U. Müller, Acta Cryst. B, 32 (1976) 582.

10 G. Schmidt and R. Boese, Chem. Ber., 109 (1976) 2148.

11 J.H. Ammeter, H.-B. Bürgi, J.C. Thibeault and R. Hoffmann, J. Am. Chem. Soc., 100 (1978) 3686; B.E.R. Schilling, B.E.R.; R. Hoffmann and D.L. Lichtenberger, ibid., 101 (1979) 585; B.E.R. Schilling, R. Hoffmann and J.W. Faller, ibid., 101 (1979) 592.

12 P.K. Baker and S.G. Fraser, Transition Met. Chem. 13 (1988) 284, and references cited therein.

13 See e.g. J.A. Pople, W.G. Schneider and H.J. Bernstein, High-resolution Nuclear Magnetic Resonance, MacGraw-Hill, New York, 1959, p. 132.

14 See e.g. D.S. Milbrath, J.G. Verkade, and R.J. Clark, Inorg. Nucl. Chem. Lett., 12 (1976) 921; E.C. Alyea, R.E. Lenkinski and A. Somogyvari, Polyhedron, 1 (1982) 130.

15 In principle, peaks due to ^{95}Mo isotopomers should also be present in the ^{31}P spectrum. To account for the temperature dependence described in the text, they must, however, have linewidths in the order of 30–100 Hz at room temperature, and this together with their low intensity (2.5% each) would make them unobservable in our spectra.

16 The resonances of other carbon atoms in the molecule should also be influenced by this effect. For all of these, however, at least one of the P-C couplings is negligible, so that "AMX" spectrum of each ^{95}Mo isotopomer consists of just two lines which coincide with the most intense lines of the AXX′ pattern. Thus, the only visible effect would be an anomalously high intensity of these lines, which was indeed observed.

17 G.M. Sheldrick, SHELXTL-PLUS Rev 2.2, Göttingen, F.R.G., 1987.

18 International Tables for X-ray Crystallography, Vol. IV, 1974, Birmingham, Kynoch Press.

19 $R = \Sigma|\Delta|/\Sigma|F_o|$, $\Delta = |F_o| - |F_c|$; $R_w = [\Sigma w \Delta^2/\Sigma w F_o^2]^{1/2}$; $S = [\Sigma w \Delta^2/(N_{obs} - N_{par})]^{1/2}$.